Journal of the European Ceramic Society 5 (1989) 209–217

Sol–Gel Coating of Silicon Nitride with Mg–Al Oxide Sintering Aid

M. Kulig, W. Oroschin & P. Greil*

Technische Universität Hamburg-Harburg, Arbeitsbereich Technische Keramik, Harburger Schloßstr. 20, D-2100 Hamburg 90, FRG

(Received 31 May 1989; revised version received 25 August 1989; accepted 28 August 1989)

Abstract

Sol–gel coating of submicron silicon nitride powder by hydroxide precipitation from bimetallic Mg–Al alkoxide in non-aqueous solution was examined. Acoustophoretic measurements in aqueous solution indicate a surface coating of the silicon nitride with a hydroxide gel layer which results in significantly higher green compact strength and improved sintering behavior as compared with the mechanically mixed powder. Due to the uniform distribution of the sintering aids, pressureless sintered compacts made from the sol–gel coated powder attained a higher density and a Weibull modulus of 17 as compared with only 5 for the mechanically mixed powder with the same composition.

In dieser Untersuchung wurden Siliziumnitridpulver über den Sol-Gel-Prozeß mit Mg–Al-Alkoxiden in nichtwässrigen Lösungen beschichtet. Akustophoretische Messungen in wässriger Lösung weisen auf eine Oberflächenbeschichtung des Siliziumnitrids mit einer Hydroxidschicht hin. Hierdurch werden erheblich höhere Grünkörperfestigkeiten und ein verbessertes Sinterverhalten gegenüber einem mechanisch gemischten Pulver erzielt. Aufgrund der homogenen Verteilung der Sinterhilfsmittel werden mit drucklos gesinterten Proben, die aus einem über den Sol-Gel-Prozeß beschichteten Pulver hergestellt wurden, höhere Dichten und ein Weibullmodul von 17 erzielt. Im Vergleich hierzu erreicht ein mechanisch gemischtes Pulver gleicher Zusammensetzung nur einen Weibullmodul von 5.

On a étudié le coating sol-gel d'une poudre de nitrure de silicium submicronique par précipitation en solution non-aqueuse de l'hydroxyde issu de l'alkoxyde bimétallique de Mg et d'Al. Des mesures acoustophorétiques en solution aqueuse indiquent une couverture du nitrure de silicium par une couche de gel hydroxyde qui entraîne une résistance mécanique de la pièce crue significativement plus élevée et un meilleur comportement au frittage que dans le cas de la poudre mélangée mécaniquement. En raison de la répartition uniforme des additifs de frittage, les compacts frittés naturellement à partir de la poudre coatée ont atteint une densité supérieure et un module de Weibull de 17 contre 5 seulement pour la poudre mélangée mécaniquement de même composition.

1 Introduction

Pressureless sintering of silicon nitride powder into dense compacts is only possible in the presence of melt-forming sintering aids which promote a liquid phase sintering process by dissolution, diffusion and reprecipitation of silicon nitride upon heating.[1] Usually, multiphase oxide mixtures of alumina, magnesia, calcia, yttria or rare earth oxides are used as sintering aids. During cooling, part of the sintering liquid is retained in the grain boundary areas as a thin glassy layer. Crystallization of the liquid and glassy phases into refractory grain boundary phases by controlled heat treatment (devitrification) has been successfully utilized to improve the high-temperature mechanical properties of silicon nitride ceramics, in particular strength, creep and slow crack growth resistance.[2] The microstructure formation during sintering of the multicomponent powder mixtures and crystallization heat treatment will, however, be essentially influenced by the uniformity of chemical composition in the starting powder. Chemical inhomogeneities such as local concentration gradients and

* To whom all correspondence should be addressed.

Journal of the European Ceramic Society 0955-2219/90/S3.50

single-phase agglomerates may generate pores and flaws upon sintering due to differential shrinkage.[3] Crystallization of ternary phases from the sintering liquid, such as $MgAl_2O_4$ (spinel), or higher component phases, for example quaternary and quinary oxynitrides,[2] may be impeded by inhomogeneous elemental distribution and large chemical gradients (diffusion paths), resulting in the formation of a high amount of residual glassy phase at the grain boundaries.

Generally, the distribution of the various powder components is achieved by mechanical mixing techniques such as ball or attrition milling. Decreasing grain size and increasing purity of newly developed silicon nitride powders, however, requires advanced powder processing techniques to avoid uncontrolled external as well as internal (particle–particle interaction) physical and chemical contamination. Colloidal processing techniques such as mixing of soluble compounds and precipitation in deflocculated and stabilized suspension may therefore provide an improved way of homogeneous distribution of sintering additives as compared to mechanical mixing of insoluble powders. Thus, a significant reduction of the necessary additive content and hence improved high-temperature properties due to a reduced content of residual intergranular glassy phase can be expected by optimum additive distribution via wet chemical mixing techniques. Such powders seem to be of particular interest for slip casting and pressing techniques, which gain increasing interest for the formation of defect-controlled and highly dense green compacts from colloidal powder mixtures.[4]

Uniform mixtures of silicon nitride powders and additive precipitates were obtained by precipitation of Mg and Y hydroxide with tetraethylammonium hydroxide from aqueous metal nitrate solutions. Samples from these mixtures showed a much greater green compact homogeneity and higher sintering densities than those prepared from the mechanically mixed powders.[5] The hydrolytic or thermal decomposition of metal alkoxides was shown to be a convenient method for homogeneously dispersing very small quantities of oxides or mixed oxides in silicon nitride. Thus, high-density silicon nitride with a minimum of Y_2O_3 or CeO_2 as the hot-pressing aid was prepared by hydrolysis of Ce or Y isopropoxide from an isopropyl alcohol solution.[6] The chemistry of alkoxide synthesis is well known and a variety of synthetic routes is described in the literature.[7] Monometallic alkoxides may be prepared under water-free conditions by direct synthesis from metals, metal halides or indirectly via alcoholysis. Bimetallic alkoxy derivatives of a number of metals have been subject of investigations dealing with the structural chemistry aspects of more complex metal alkoxides.[8] Ultrapure $MgAl_2O_4$, for example, could be prepared from liquid (25°C) double alkoxides of the type $MgAl_2(OR)_8$, where the secondary alkoxy group contained 4 to 7 carbon atoms.[9] Double alkoxides as homogeneous molecular compounds may provide the appropriate state of metal mixture on a molecular scale combined with potential surface active properties in non-aqueous solutions. The dispersability of silicon nitride powder in n-C_6H_{14} was shown to be significantly improved by specific adsorption of Al-(iOPr)$_3$ on the Si_3N_4 particle surfaces.[10] A γ-alumina coating layer was formed via a surface ester reaction of silanol groups on the Si_3N_4, resulting in a shift of the isoelectric point (iep) from pH 5·2 to 8·2. Amorphous spinel layers were obtained by dip coating in an isopropanol solution of Mg–Al-isopropoxide, where the precipitation of hydroxide was controlled by diethanolamine.[11]

It was the aim of this work to investigate the sol-gel coating of submicron silicon nitride powder with bimetallic Mg–Al oxide. The preparation of the Mg–Al butoxide in alcoholic solution from which the hydroxide was precipitated into deflocculated silicon nitride suspension will be described. The distribution of the precipitated hydroxide was examined by acoustophoretic measurements. This novel technique may be used for higher concentrated suspensions to characterize the surface chemistry of the solvated solid phase. Both the precipitation mixed and the mechanically mixed powder mixtures were sintered under equal conditions and the resulting strength values were statistically evaluated to describe the influence of processing technique on the microstructure-dependent property variations.

2 Experimental Procedure

2.1 Mg–Al-alkoxide preparation

High-purity Mg metal and liquid $Al(OC_4H_9)_3$ were used to prepare $MgAl_2(OC_4H_9)_8$ in isobutylalcohol. Mg powder (6·3 g, 0·26 mol) and 128 ml of liquid $Al(OC_4H_9)_3$ (0·5 mol) were reacted in nitrogen atmosphere with 38·5 g of C_4H_9OH (0·52 mol) in a molar mixture of 1·02:2:2·05 in water-free toluene under reflux for 8 h, according to the reaction

$$Mg + 2Al(OC_4H_9)_3 + 2C_4H_9OH \rightarrow MgAl_2(OC_4H_9)_8 + H_2 \quad (1)$$

until hydrogen release ceased. A small excess of Mg and isobutylalcohol is necessary to avoid residual Al alkoxide. $MgAl_2(OC_4H_9)_8$ remained after evaporation of the toluene/butanol mixture under reduced pressure as a highly viscous and clear liquid. Subsequently, the double-alkoxide was slowly hydrolyzed in air, according to the reaction

$$MgAl_2(OC_4H_9)_8 + 8H_2O \rightarrow MgAl_2(OH)_8 + 8C_4H_9OH \quad (2)$$

with the hydroxide precipitating as a white powder. After removing the alcohol by distillation, the hydroxide reaction product was subjected to thermogravimetric analysis (STA 409, Netzsch Gerätebau, Selb, FRG) up to 1200°C. Complete calcination (dehydration) of the Mg–Al hydroxide finally resulted in the formation of the cubic spinel phase:

$$MgAl_2(OH)_8 \rightarrow MgAl_2O_4 + 4H_2O \quad (3)$$

2.2 Powder processing

A high-purity α-Si_3N_4 powder (LC 12, H.C. Starck, Berlin, FRG), with a specific surface area (BET) of 19·8 $m^2 g^{-1}$ and a mean grain size (FSSS) of 0·45 μm, was used for the powder processing experiments. The major impurities in the starting silicon nitride powder were C and O with 0·19 and 1·98 wt%, and a total metal content (Fe + Al + Ca) of 0·048 wt%. Blending of the Si_3N_4 powder with 5, 10 and 15 wt% of the additives was achieved either by mechanical mixing (*mm*) of the presynthesized oxide or by in-situ precipitation (*pm*) of the hydroxide in alcoholic Si_3N_4 suspension.

Mechanical mixing was carried out in an attrition mill filled with Al_2O_3 balls for 4 h at 500 rev/min in isopropanol. After milling, the powder mixture was dried in a rotary evaporator, sieved with 100 μm and cold isostatically pressed into cylindrical pellets (10 × 10 mm) or rectangular bars of 4 × 4 × 40 mm^3 at a pressure of 700 MPa. The green density was determined from the bar geometry.

Mixing by in-situ precipitation of the hydroxide in isobutyl alcohol suspension required the presence of a well-deflocculated system. To achieve deflocculation, the pure silicon nitride powder was first ultrasonicated for 30 min. The appropriate amount of liquid alkoxide was added under intensive stirring. Subsequently, H_2O/triethylamine solution was slowly dropped into the suspension, which was stirred for 6 h to assure complete precipitation of the hydroxide. The solvent was removed under slight vacuum at room temperature in a rotary evaporator. The dried powder was calcined at 1000°C for 1 h. Larger agglomerates that had been formed during calcination were destroyed by ball milling the powder in isopropanol for 4 h. Finally, the *pm* powder was dried, sieved with 100 μm and pressed under identical conditions as for the *mm* powder.

X-ray diffraction for phase analysis of the calcined products was carried out with monochromated $Cu_{K\alpha}$-radiation (PW 1820, Philips, Eindhoven, Netherlands). Green and sintered compacts were analysed by SEM (Stereoscan S-200, Cambridge Instruments, UK) after coating the surfaces with a thin layer of gold. The distribution of Mg and Al in the processed powder mixtures was evaluated by chemical mapping analysis. A wavelength dispersive chemical analysis system (WDX) equipped with a TAP detector was used, with a scanning time of 5 min.

2.3 Acoustophoretic measurements

Depending on the distribution and morphology of the additive phase in the Si_3N_4 powder mixture, different surface charges will result which may severely influence the colloidal processing behavior, with respect to green compact formation by dry powder pressing or slurry casting techniques. The effective surface charge which dominates the rheological properties may be characterized by measurement of the particle mobilities from which zeta potentials may be derived.[12] An acoustophoretic measurement technique (PEN KEM 7000, PEN KEM Inc., Bedford Hills, New York) was used to determine relative acoustophoretic mobilities (*RAM*). During the measurement the charged particles are subjected to a compressional ultrasonic wave of 200 kHz which gives rise to a periodic polarization of the ionic atmosphere surrounding the particles. The resulting alternating potential (colloid vibration potential, *CVP*) can be measured, from which the so-called relative acoustic mobility (*RAM*) is derived. The *RAM* can be converted to an acoustic mobility, *AM*, under consideration of the particle volume fraction, ϕ, and the densities of the liquid, ρ_1, and solid phase, ρ_2:[13]

$$AM = \frac{RAM}{2\phi}\left[\frac{\rho_1}{\rho_2 - \rho_1}\right]\frac{\gamma(\kappa a, \phi)}{\Omega(\phi)} \quad (4)$$

$\gamma(\kappa a, \phi)/\Omega(\phi)$ is a complex function which takes into account the particle–particle electrical and hydrodynamic interactions in concentrated suspensions based on the cell model theory.[14,15] For thin double layers ($\kappa a \gg 1$), however, this interaction parameter can be approximated by $(1 - \phi)$,[16] so that for decreasing particle concentrations it tends to unity. For the acoustophoretic measurements the

powder was dispersed in aqueous solution at 25°C and an ionic strength of 0·01 mollitre^{-1} KCl. Thus, the reciprocal Debye length, κ, in the KCl solution is $\approx 3{\cdot}3 \times 10^8\ m^{-1}$, and taking into account the mean grain size of the silicon nitride powder, a, as $\approx 4{\cdot}5 \times 10^{-7}$ m, a normalized double layer thickness of $\kappa a \simeq 148$ results.[17] From the acoustic mobility the zeta potential, ζ, can be determined using similar relations as for electrophoretic mobility measurements. The zeta potential, ζ, was calculated from the acoustophoretic mobility and the Helmholtz–Smoluchowski equation,[17] which is valid for large $\kappa a > 100$:

$$\zeta = AM\frac{\eta}{\varepsilon} \tag{5}$$

η and ε are the viscosity and dielectric constant for water at 25°C (0·89 mPa s and $6{\cdot}95 \times 10^{-10}$ $C^2 J^{-1} m^{-1}$). The mobility measurements were carried out in suspensions with solid concentrations of 1 vol% (3·1 wt%). A titration burette was used to change the pH in the range 2–12 by adding 1 M KOH or HCl, respectively. Prior to taking the measurements, the suspension was ultrasonicated and magnetically stirred under vacuum to ensure that only single particles were measured.

2.4 Sintering and strength evaluation

A gas pressure furnace equipped with carbon heating elements was used for sintering the Mg–Al oxide doped specimens in a nitrogen atmosphere at a maximum pressure of 2 MPa. The specimens were embedded in Si_3N_4 powder. Linear heating rates were applied up to the final temperature of 1900°C, and no isothermal period was reached. The three major sections of the sintering schedule involved (i) a rapid heating up to 1200°C in vacuum within 60 min, (ii) a heating period from 1200 up to 1800°C with a linear heating rate of 10 K min^{-1} at 0·2 MPa and (iii) a soaking period with a linear but slow heating rate of 1·7 K min^{-1} up to 1900°C. During the temperature increase from 1800 to 1900°C, the nitrogen pressure was simultaneously increased from 0·2 to 2 MPa in order to prevent silicon nitride decomposition. After cooling, weight change, total shrinkage and density were measured.

Rectangular bars of $4 \times 4 \times 40\ mm^3$ were cut with diamond and polished with diamond paste 1 μm. Strength was determined by four-point bending with 12/30 mm span and a crosshead speed of 0·1 mm min^{-1}. From the strength data mean values and the Weibull parameter were derived from at least 15 specimens. The critical defect sizes were measured microscopically on the fractured surfaces. The defect sizes were arranged in classes of 50 nm to establish frequency and cumulative frequency curves.

3 Results and Discussion

3.1 Powder coating

Thermal balance analysis of the Mg–Al hydroxide precipitate showed that the dehydration of the hydroxide was almost completed below 600°C. A total weight loss of approximately 60 wt% was found, which satisfactorily corresponds to the ideal $MgAl_2(OH)_8$ composition with a theoretical weight loss of 63 wt%. Thus, for the sol-gel coating experiments the powder mixtures were calcined at 1000°C for 1 h. X-ray analyses of the hydrolysed alkoxy products after calcination in air at 1000°C for 1 h reveal the formation of single-phase $MgAl_2O_4$, whereas after annealing at 1200°C Al_2O_3 was found as an additional crystalline product, which indicates an increasing loss of Mg when the calcination temperature was raised. Estimation of the primary crystallite size from X-ray line broadening according to the Scherrer equation reveals an initial size of approximately 15 nm after calcination at 1000°C and 30–40 nm at 1200°C of the separately prepared oxide powder. Supposing that the Si_3N_4 particles would be coated with a dense spinel layer, a mean layer thickness of 5–20 nm is calculated for 5–15 wt% of oxide additive. However, a uniform coating will only be possible with an oxide particle size smaller than the layer thickness. Therefore, the *pm* powders were calcined at a maximum temperature of 1000°C.

In Figs 1(a)–(d) are shown SEM micrographs and the corresponding distribution of Mg and Al of cold isostatically pressed silicon nitride powder mixtures. While at low magnifications the standard deviation of the WDX spectrum for different areas examined is low, and is associated with the counting statistics, large deviations of the spectrum may occur at high magnifications.[4] Although the area examined will not be representative of the whole microstructure, large differences in spot density represent different states of phase uniformity between the *pm* and *mm* powders. The high spot densities observed in the *pm* powder (Figs 1(b) and (d)) may be associated with the presence of $MgAl_2O_4$ on the nitride particle surface, whereas the low spot densities in the *mm* powder (Figs 1(a) and (c)) may be related to an inhomogeneous elemental distribution and shading effects of nitride and oxide particles in the scanned area. Thus, from the chemical mapping of the Mg and Al distribution an extremely uniform

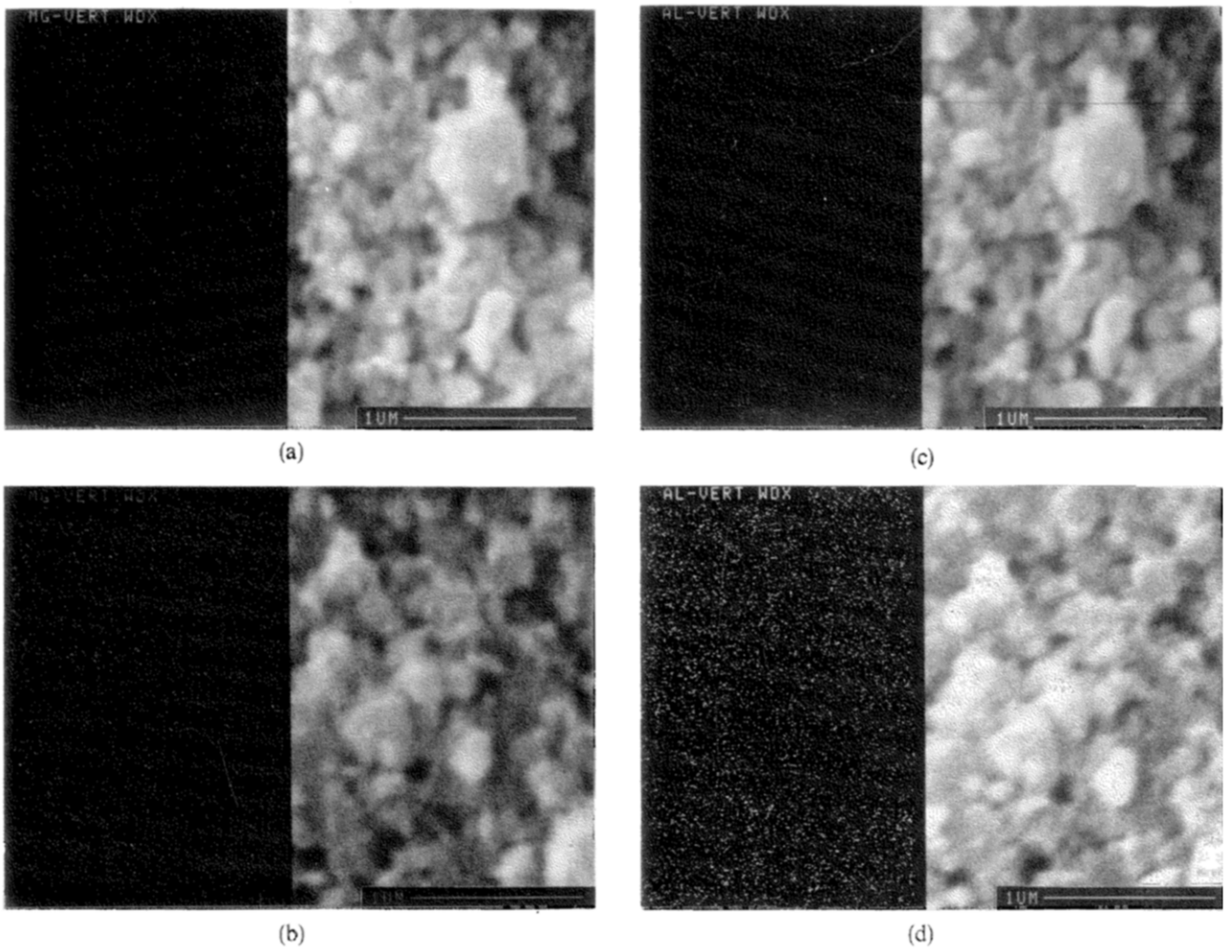

Fig. 1. SEM micrographs of the cold isostatically pressed powder mixtures: (a) *mm*, Mg distribution; (b) *pm*, Mg distribution; (c) *mm*, Al distribution; and (d) *pm*, Al distribution.

distribution of the sintering additive on the particle scale may be concluded in the *pm* powder, whereas the *mm* powder may be characterized as a chemically homogeneous material on the agglomerate size range only.

In-situ precipitation of the hydroxide into the alcoholic silicon nitride suspension may be described by a multistep process involving (i) the formation of an initial alkoxide surface layer by chemical adsorption and (ii) growth of the surface layer by a gel polymerization process upon hydrolysis.[10] A surface reaction involving a nucleophilic attack of the oxygen in the alkoxy group on the silicon atom is supposed to result in an ester formation reaction according to

$$\equiv Si\text{–}OH + RO\text{–}Al(OR)_2 \rightarrow \equiv Si\text{–}O\text{–}Al(OR)_2 + ROH \quad (6)$$

In Fig. 2 is shown a schematic model for $MgAl_2(OR)_8$ chemisorption ($R = C_4H_9^+$), which is based on the proposed molecular structures of Al alkoxides.[8] Various types of di-, tri- and tetrameric clusters of the $Al(OR)_3$ with $R = C_3H_7$ or C_4H_9 are characterized by a bidentate ligand structure of the alkoxide group:

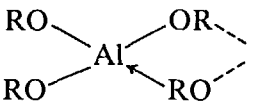

It may be possible that a second metal atom such as Mg may link these clusters to form a bimetallic alkoxide layer on the silicon nitride surface. Bimetallic or mixed alkoxides are therefore of particular interest for improving the homogenous distribution of complex oxide additives by surface adsorption processing techniques in non-aqueous solutions.

Hydrolysis reaction upon water addition links the alkoxide molecules by a polymerization type of sol-gel reaction. The thickness of the hydroxide layer may be controlled by the alkoxide concentration, the water 1:1 alkoxide ratio and the precipitation conditions.[11] The total amount of additive will then be mainly determined by the precipitate layer

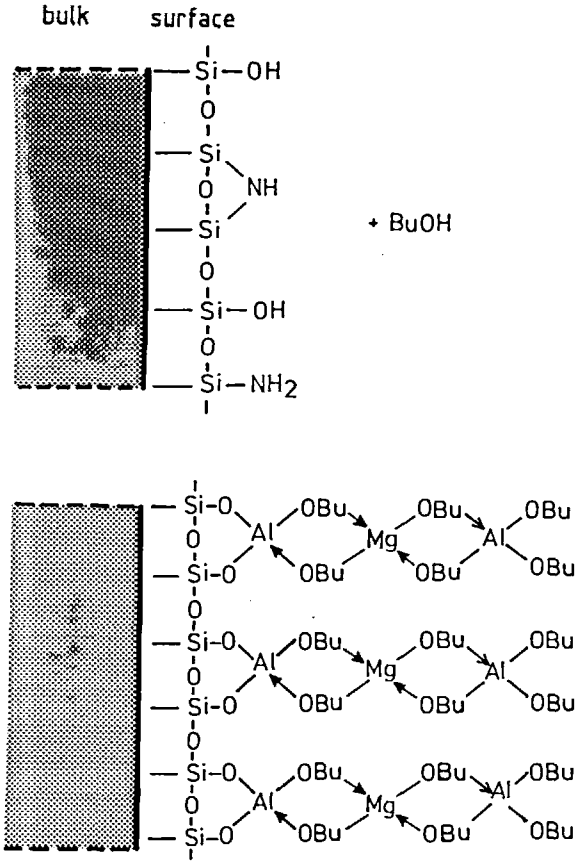

Fig. 2. Schematic model of the $MgAl_2(OC_4H_9)_8$ chemisorption on a silicon nitride surface: (a) the unpurified silicon nitride surface in alcoholic suspension; (b) bonding of the alkoxide molecules via oxygen bridging on to the purified silicon nitride surface.

thickness and the silicon nitride grain size, although an unknown amount of precipitate may be formed by homogeneous nucleation. To avoid the formation of isolated hydroxide precipitates and hydroxide bonded agglomerates the alkoxide-coated silicon nitride powder may be directly calcined or transferred to a slip casting process without any hydrolysis reaction. The surface adsorbed alkoxide layer will transform to the corresponding oxide layer upon decomposition of the alkoxide:

$$MgAl_2(OR)_8 \rightarrow MgAl_2O_4 + (CH_x, H_2O, CO) \quad (7)$$

3.2 Colloidal stability

In Fig. 3 are shown the zeta potentials of the as-received silicon nitride and the Mg–Al oxide (10 wt%) containing powder mixtures in the pH range 2–12. While the as-received silicon nitride reveals an isoelectric point, iep, ($\zeta = 0$) at pH 7·4, the *mm* powder exhibits the iep at pH 9·2 and the *pm* powder at 10. At pH values above the iep a negative, whereas at lower pH a positive, surface charge is established on the silicon nitride particles, due to the adsorption of hydroxyls or protons onto an amphoteric silanol group:[18]

$$[Si\text{–}OH_2]^+ \xleftarrow{H^+} [Si\text{–}OH] \xrightarrow{OH^-} [Si\text{–}O]^- + H_2O \quad (8)$$

In the processed powder containing 10 wt% of Mg–Al oxide additives the surface charge is generated by the metal hydroxide surface sites of Mg and Al. The formation of a positive surface charge at intermediate and low pH will be dominated by the dissociation of basic Mg–OH ($pK_b = 2{\cdot}6$) and Al–OH ($pK_b = 2{\cdot}8$) sites on the particle surface:

$$[(Mg, Al)\text{–}OH] \xrightarrow{H_2O} [(Mg, Al)(OH_2)]^+ + OH^- \quad (9)$$

which is essentially equivalent to the adsorption of protons.[12] Specifically adsorbed ions can be recognized by their ability to reverse the sign of the zeta potential, whereas indifferent ions can only reduce the zeta potential asymptotically to zero.[19] Thus, the shift of the iep to higher pH values indicates a chemical adsorption of cations on the charged surface.

The relatively small deviations of the *mm* powder from the as-received silicon nitride (Fig. 3) indicate that the surface of the oxide particles as well as the free surface of the silicon nitride powder contribute to the experimentally measured zeta potential. The effect of pH on the zeta potential of silicon nitride and oxide powder mixtures in concentrated suspensions can be explained in terms of the total surface area of each powder present in the dispersion, as it was shown for alumina and titania mixtures.[20] The greater difference of the zeta potential curve of the

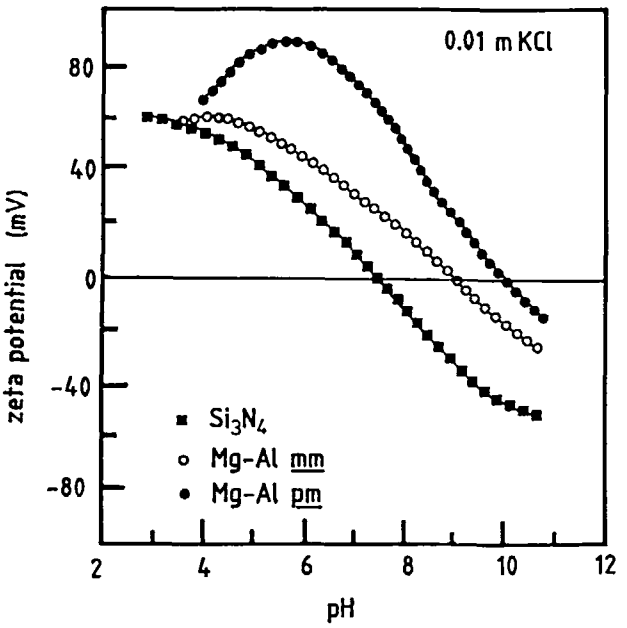

Fig. 3. Zeta potential of the as-received silicon nitride powder and the *mm* and *pm* powders containing 10 wt% $MgAl_2O_4$.

pm powder, however, as compared to the *mm* powder, may be attributed to the effect of a coating of the silicon nitride particles with the oxide layer which dominates the surface charge formation. The iep and the Ψ_ζ-pH-dependence of the *pm* powder equals that of pure $MgAl_2O_4$ powder which was measured under identical conditions. The zeta potential of the coated powder may then be described by an adsorption–precipitation mechanism of hydrolysed cations (eqn (9)) which was proposed in order to explain the electrokinetic behavior of silica particles dispersed in a solution containing hydrolyzable cobalt ions.[21] The *pm* powder may then be addressed as a single-phase powder, from which well deflocculated suspensions may be formed at significantly lower pH than from the silicon nitride powder.

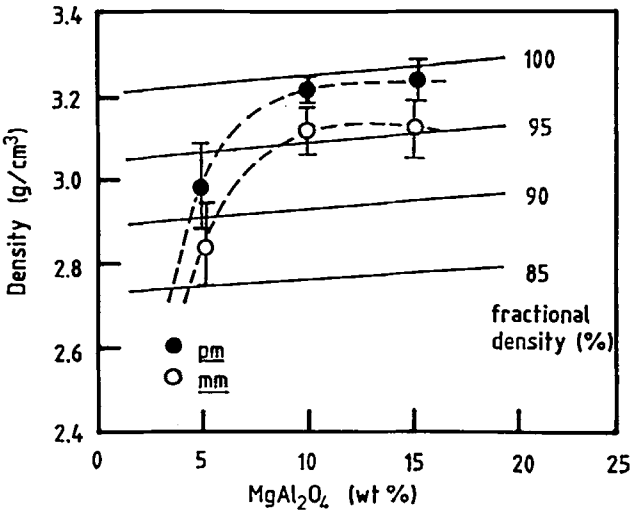

Fig. 4. Density after pressureless sintering (1900°C) of silicon nitride as a function of the $MgAl_2O_4$ content and the powder processing route.

3.3 Sintering and strength

The green densities of the cold isostatically pressed powder mixtures show slight differences between the mechanically and precipitation mixed powders, respectively. While the *mm* powder attained densities of approximately 63–63·5% th.d., the *pm* powder reached only 61–61·5%. Although the green density of the coated silicon nitride powder was lower, the green compact strength attained $27{\cdot}1 \pm 3{\cdot}1$ MPa, as compared to $9{\cdot}7 \pm 2{\cdot}2$ MPa for the mechanically mixed powder.

Distinct differences were found for the sintering behavior of the differently processed powders. Earlier investigations have shown that at least 15 wt% of $MgAl_2O_4$ was necessary to obtain a maximum fractional density of 95–96% by pressureless sintering of mechanically mixed powders.[22] The sintering density versus the $MgAl_2O_4$ concentration found in this work is shown in Fig. 4. Generally, the coated powder yields higher densities than the mechanical mixtures so that lower amounts of sintering additives can be used. The *pm* powder containing 10 wt% of sintering aid attained a density of 3·20 g cm^{-3} ($\simeq$98·5% of the theoretical density, 3·25 g cm^{-3}), while the *mm* powder reached only 3·12 g cm^{-3} ($\simeq$96%). Thus, the *pm* powder showed a 10% higher volume shrinkage as compared to the *mm* powder upon sintering. These differences are to be related to the characteristic distribution of the additives, because the amount and composition of the additives, as well as the sintering programme, were kept constant for all specimens. An enhancement of sintering was also observed in yttria-doped silicon nitride when the additives were introduced to the powder compact by an hydroxide precipitation process from salt solution.[5] A similar effect of improved chemical homogeneity on sintering was reported from earlier experiments where silicon nitride was sintered with additions of MgO, Al_2O_3 and $MgAl_2O_4$.[23] It was found that the latter resulted in better sintering behavior than either of its components or their equimolar mixture.

From the strength measurements a mean fracture stress of 555 ± 31 (5·6%) MPa was determined for the *pm* samples and 438 ± 95 (21%) MPa for the *mm* samples. The corresponding fracture probability versus fracture stress curves, according to the Weibull statistics, are shown in Fig. 5. From the slope of the Weibull curves the characteristic

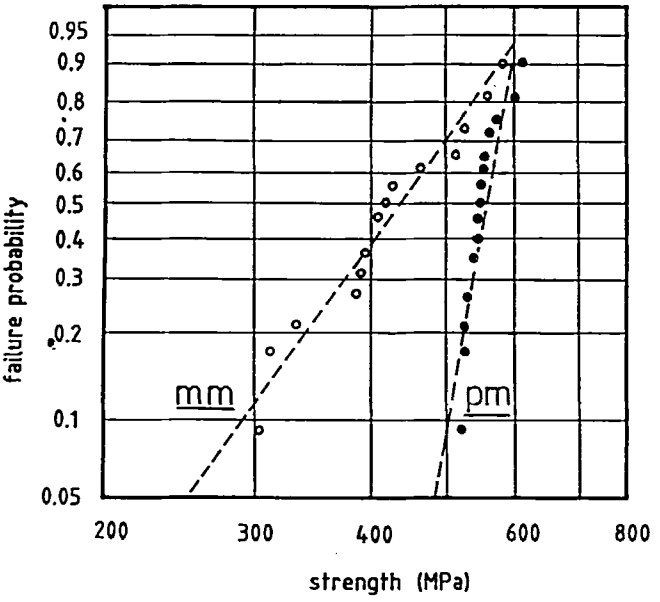

Fig. 5. Failure probability diagram (Weibull plot) of the sintered specimens containing 10 wt% $MgAl_2O_4$.

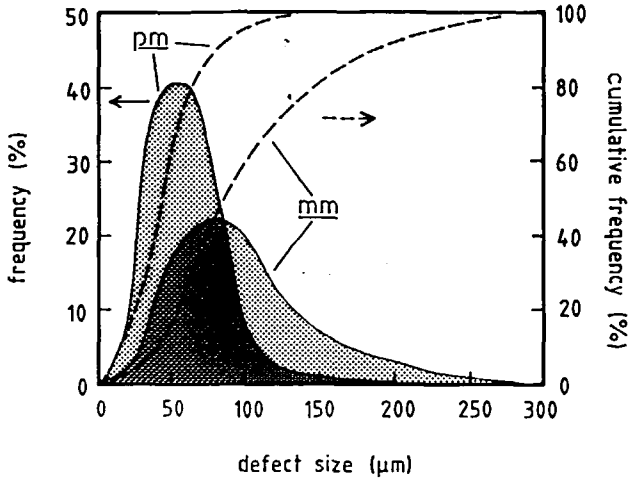

Fig. 6. Size distribution function (frequency) and density function (cumulative frequency) of the critical defect sizes in the broken specimens.

parameter m was determined. Again, the *pm* samples show a significantly higher value of 17, as compared to 5 for the *mm* samples. The significantly higher Weibull modulus of the *pm* samples is reflected in a narrow distribution of the critical defect sizes as measured from the fracture surfaces of the broken specimens. In Fig. 6 are shown the size distribution function (frequency) and the density function (cumulative frequency) of the critical defects which were observed at or near the tensile surface. More than 40% of the defects analysed in the broken *mm* samples are $>100\,\mu$m in size, whereas less than 5% are above this value in the *pm* samples.

Assuming the defect distribution in the sintered compact to be related to the agglomerate structure in the starting powder mixture, the correlation between the defect size distributions and the applied powder processing routes clearly indicates the importance of chemical homogeneity in addition to the physical uniformity of low agglomerated powder constitutents in sinterable silicon nitride. The SEM micrographs given in Figs 7(a) and (b) show fracture surfaces of the *mm* and *pm* samples. While the *pm* sample reveals an extremely homogeneous microstructure, pores and microstructural heterogeneities could generally be found in the *mm* samples. An

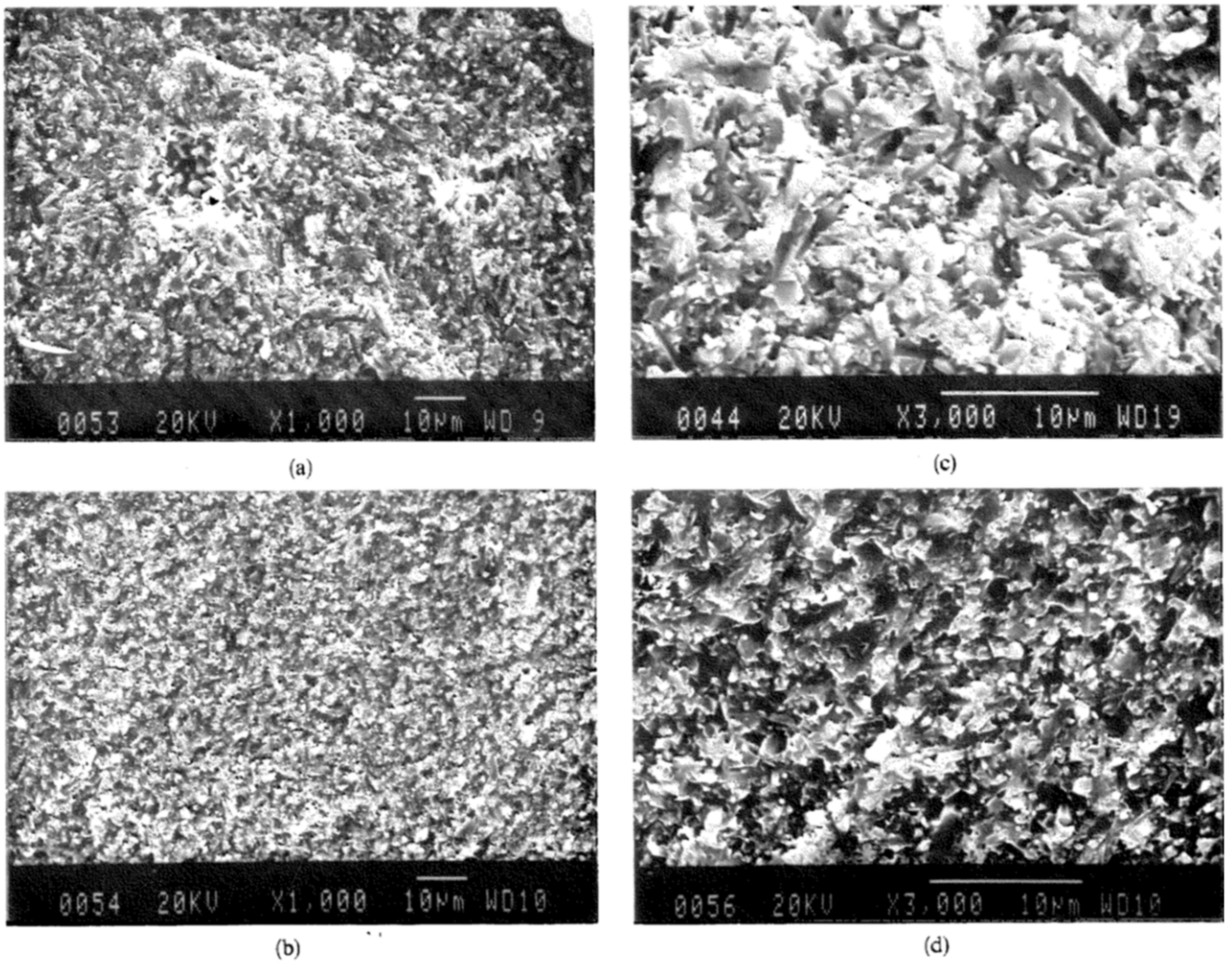

Fig. 7. SEM micrographs of fracture surfaces of the (a, c) *mm* and (b, d) *pm* samples.

intergranular fracture mode appeared to dominate the fracture behavior of both samples. The fracture in both specimens initiated from isolated pores, the size of which, however, is significantly larger than the grain size scale (Fig. 6). The formation of these large pores may be attributed to the incorporation of single-phase hydroxide agglomerates which were formed during *in situ* precipitation. Comparing the grain size of the elongated silicon nitride particles, significant differences are shown in Figs 7(c) and (d) between both samples. Grains up to 10 μm in length could be found in the *nm* samples but only half of this grain size could be detected in the *pm* samples. The retainment of a smaller grain size during pressureless sintering in the *pm* samples due to a uniform elemental distribution may lead to improved bend strength, provided that the introduction of large hydroxide agglomerates during *in situ* precipitation can be avoided.

4 Conclusions

Generally, the precipitation mixing of sintering additives by sol-gel coating of silicon nitride powder results in a better elemental distribution as compared to mechanical mixing. The attractive advantages of precipitation or adsorption mixing seem to be:

(1) Reduction of the amount of liquid forming sintering additives, which is necessary to obtain full densification upon pressureless sintering;
(2) Reduction of the sintering temperatures due to reduced diffusion distances and intimate mixture of elements in the additive phase;
(3) Improved properties for colloidal filtration techniques because of single-phase behavior dominated by the highly chargeable hydroxide/oxide layer;
(4) Control of oxygen contamination due to screening of the oxidation and hydrolysis-sensitive silicon nitride surface.

The processing properties for colloidal filtration techniques such as slip casting and colloidal pressing techniques may significantly be improved by using surface-coated silicon nitride. As a result of the improved green compact microstructure the scattering of the properties of the sintered material will be reduced. Thus, the reliability of the material properties, which is considered as a key aspect for the applicability of high-performance ceramics, may be improved.

Acknowledgement

H. Labitzke, from the Max-Planck-Institute for Metals Research, Stuttgart, FRG, is gratefully acknowledged for SEM and chemical mapping analyses.

References

1. Weiss, J. & Kaysser, W. A., In *Progress in Nitrogen Ceramics*, ed. F. L. Riley. Nijhoff, Boston, Mass., 1983.
2. Greil, P. *Sci. Ceram.*, **14** (1987) 645.
3. Raj, R. & Bordia, K., *Acta Metall.*, **32** (1984) 1003.
4. Lange, F. F., *J. Am. Ceram. Soc.*, **72** (1989) 3.
5. Shaw, T. M. & Pethica, B. A., *J. Am. Ceram. Soc.*, **69** (1986) 88.
6. Mah, T.-I., Mazdiyasni, K. S. & Ruh, R., *Ceram. Bull.*, **58** (1979) 840.
7. Okamura, H. & Bowen, H. K., *Ceram. Int.*, **12** (1986) 161.
8. Mehrota, R. C. & Mehrota, A., *Inorg. Chim. Acta*, **5** (1971) 127.
9. Thomas, I. M., US Patent No. 3786137, 15 January 1974.
10. Kishi, K., Umebayashi, S., Pompe, R. & Persson, M., *J. Ceram. Soc. Jpn.*, **96** (1988) 698.
11. Takahashi, Y. & Naganawa, H., *Yogyo Kyokai Shi*, **95** (1987), 1107.
12. Hunter, R. J., *Zeta Potentials in Colloid Science.* Academic Press, London, 1981.
13. Marlow, B. J., Fairhurst, D. & Pendse, H. D., *Langmuir*, **4** (1988) 611.
14. Levine, S., Neale, G. & Epstien, J., *J. Colloid Interface Sci.*, **57** (1976) 424.
15. Kuwabara, S., *J. Phys. Soc. Jpn.*, **14** (1959), 527.
16. Zukowski, C. F. & Saville, D. A., *J. Colloid Interface Sci.*, **115** (1987), 422.
17. Hiemenz, P. C., *Principles of Colloid and Surface Chemistry*, Dekker, New York, 1986.
18. Greil, P., Nagel, A., Stadelmann, H. & Petzow, G., In *Proc. 3rd Int. Conf. Cer. Mat. and Comp. for Engines*, Las Vegas, Nevada, 1988.
19. Modi, H. J. Fürstenau, D. W., *J. Phys. Chem.*, **61** (1957) 640.
20. Rao, A. S., *Ceram. Int.*, **14** (1988) 71.
21. James, R. O. & Healey, T. W., *J. Colloid Interface Sci.*, **40** (I–III) (1972) 42, 53, 65.
22. Rabinovich, E. M., Harel, L. & Fischer, R., *Special Ceramics*, **7** (1981) 71.
23. Masaki, H. & Kamigaito, O., *J. Ceram. Soc. Jpn.*, **84** (1976) 508.